Available online at www.sciencedirect.com
SCIENCE DIRECT
Journal of Colloid and Interface Science 278 (2004) 53–62
JOURNAL OF Colloid and Interface Science
www.elsevier.com/locate/jcis

Mechanical properties and stability measurement of cholesterol-containing liposome on mica by atomic force microscopy

Xuemei Liang, Guangzhao Mao, K.Y. Simon Ng *

Department of Chemical Engineering and Materials Science, Wayne State University, 5050 Anthony Wayne Drive, Detroit, MI 48202, USA

Received 4 November 2003; accepted 21 May 2004

Abstract

The micromechanical properties of pure and cholesterol modified egg yolk phosphatidylcholine (EggPC) vesicles prepared by sonication were studied by atomic force microscopy (AFM) on mica surface. The force curves between an AFM tip and an unruptured vesicle were obtained by contact mode. During approach, two repulsion regions with two breaks were observed. The slopes of the two repulsive force regimes for the pure EggPC vesicles are determined to be several times lower than that of EggPC/cholesterol vesicles. The elastic properties from force plot analysis based on the Hertzian model showed that Young's modulus (E) and the bending modulus (k_c) of cholesterol-modified vesicles increased several-fold compared with pure EggPC vesicles. The significant difference is attributed to the enhanced rigidity of the EggPC vesicles as a result of the incorporation of cholesterol molecules. The behavior of cholesterol-modified vesicles upon adsorption is different from that in solution as revealed by mechanical properties. The results indicate that AFM can provide a direct method to measure the mechanical properties of adsorbed small liposomes and to detect the stability change of liposomes.

Keywords: Unilamellar small vesicle; Bending modulus; Young's modulus; Atomic force microscopy

1. Introduction

Liposomes show potential as novel carriers for drug molecules, proteins, nucleotides, plasmids, etc. In addition there is a broad spectrum of non-medical applications such as cosmetics and biosensors [1–3]. However, the aqueous dispersion of liposomes is metastable; therefore stability of vesicles is a major concern for various types of vesicular applications. For example, short blood circulation time due to liposome instability as a drug carrier will affect the effective access to and interaction with the target [4].

In addition to stabilization by polymerization or by polymer insertion [5–9], incorporation of cholesterol is also known to affect liposome interaction and bilayer stability [10–15]. By varying the amount of cholesterol in small unilamellar dipalmitaylphosphatidylglycerol (DPPG) vesicles, Virden and Berg [11] found that cholesterol improved vesicle resistance to aggregation. Liu et al. [12] compared the structure of the bilayer and the interaction force between the liposomes and demonstrated that the physical stability of liposome can be enhanced by cholesterol addition. Cholesterol increased the absolute zeta-potential and electrostatic repulsion between PC liposomes. It was found that 11 mol% cholesterol incorporated into the dipalmitaylphosphatidylcholine (DPPC) bilayer would reduce the van der Waals attraction force and increase the net repulsion forces between bilayers [13]. The fluidity or intravesicle interactions of liposomes are also changed by cholesterol addition. It was shown that phosphatidylcholine (PC) vesicles are more rigid and sustain more severe shear stress after introducing cholesterol [14]. The maximum amount of cholesterol that can be incorporated into reconstituted bilayers is widely assumed to be about 50 mol%, although the solubility limit for cholesterol in lipid shows a subtle dependence on lipid molecular structure [15].

There is an increasing trend toward studies of lipid/cholesterol bilayer systems, while studies of cholesterol in bilayers have usually focused on the intravesicle interactions, which affect aggregation and fusion processes. Several interesting aspects related to mechanical properties, namely, the cohesion interaction between cholesterol and lipid, the

* Corresponding author. Fax: 313-577-3810.
E-mail address: sng@wayne.edu (K.Y.S. Ng).

0021-9797/$ – see front matter
doi:10.1016/j.jcis.2004.05.042

mechanical stiffness of membranes, and their effect on membrane permeability to water, remain to be fully elucidated and quantified [15].

The mechanical properties of phospholipid membranes can be related to many aspects of the behavior of phospholipid vesicles, such as their formation, stability, size, shape, fusion, and budding processes [16]. Bending modulus is a characteristic property of the vesicles that is closely related to the activities of liposomes and the gel–liquid phase transition of a liposome's bilayer membrane. A number of experimental methods have been designed to measure the bending rigidity of the membrane, such as shape fluctuation recorded by microscopy [17–19], micropipette suction [15], micropipette aspiration, and so on [20]. However, it should be noted that the values of bending modulus obtained by these techniques scatter strongly. Sometimes the same technique applied by different research group yields significantly different bending modulus values [16]. Furthermore, these techniques work well for much larger vesicles (usually several micrometers) suspended in solution. Since membranes are extremely flexible, well-characterized local force and sub-micrometer detection of the membrane deformation of individual vesicles are required to measure the local bending modulus. Thus, the ability to characterize and to tailor the stability of the micromechanical properties of individual liposomes, especially on a substrate surface, remains a major challenge.

Atomic force microscopy (AFM) is a unique technique that can directly probe the elastic properties of many surfaces using force plots [21,22], in which the AFM tip moves up and down over a point on the sample surface, probing the elastic and adhesive properties of materials or force mapping [23–27], giving a complete elastic properties maps of heterogeneous samples. The Young's modulus (E_{ves}) of the *Torpedo* synaptic vesicles with apparent diameters of around 90–150 nm were explored by Laney et al. [24] from force mapping by averaging approach and retraction force curves. However, they did not observe any break points in the force curves that can provide additional information related to the structure of vesicles. AFM study of individual vesicles remains challenging due to the small size and softness of vesicles, vesicle size distribution, and possible artifacts induced by the AFM tip.

More recent liposome investigations mostly use homogeneous unilamellar vesicles in the size range 50–150 nm because this size range is a compromise between loading efficiency of liposomes (which increases with increasing size), liposome stability (which decreases with increasing size), and ability to extravasate (which decreases with increasing size) [3]. Our approach is to use the force measurement capability of atomic force microscopy to study the effect of cholesterol on vesicles by obtaining the local elastic constants of individual small unilamellar vesicles on a substrate. In our previous study, the morphology and micromechanical properties of small EggPC vesicles on mica by AFM force plots were reported [28].

In this paper, our objective is to demonstrate that AFM can be used to investigate the effects of cholesterol concentration on the micromechanical properties of the small unilamellar EggPC liposomes adsorbed on mica. EggPC lipid was chosen since stable vesicles on flat mica surface without fusion were observed by AFM [29]. We will show that AFM force curves can directly measure local elastic properties of small vesicles at the solid–liquid interface. Moreover, our results indicate that the behavior of cholesterol-modified vesicles on mica surface is very different from that in solution.

2. Materials and methods

2.1. Materials

Egg yolk phosphatidylcholine (EggPC) and cholesterol with 99% purity purchased from Sigma (St. Louis, MO) were used in this study. Sodium salt, chloroform, methanol, and acetone were purchased from Fisher Chemicals (Fairlawn, NJ). Grade 2 muscovite ruby mica from Mica New York (New York, NY) was used as substrate because it is molecularly smooth. In aqueous solutions, mica cleavage surface becomes negatively charged. Deionized water with resistivity 18 MΩ cm was obtained from a Barnstead Nanopure water purification system (Dubuque, IA). All the glassware used in this study was cleaned and rinsed thoroughly with water prior to use.

2.2. Preparation of the lipid vesicles suspension solution

Multilamellar vesicles (MLVs) solution was obtained by dissolving appropriate amounts of EggPC lipids and cholesterol in chloroform/methanol (2:1 v/v) and evaporating the solvent with nitrogen [30]. After a further 30 min of drying in a desiccator connected to a rotary vacuum pump, the lipid mixtures were hydrated by stirring in a buffer solution (20 mM NaCl in pure water). Small unilamellar vesicles (SUVs) were produced from the MLV suspension by sonication to clarity (about 1 h) in a Branson 2200 bath sonicator (Danbury, CT). The suspension was kept in an ice bath during the sonication process. Sonicated samples were centrifuged for one hour at 16,000 rpm to remove large lipid fragments in a Sorvall OTD70B ultraspeed centrifuge (Wilmington, DE).

2.3. Light scattering

The particle size distribution of vesicles in buffer solution (20 mM NaCl) was measured using Nicomp 380 ZLS light scattering instrument (Santa Barbara, CA). Polystyrene with 32 ± 1.3 nm diameter nanosphere TM size standards from Duke Scientific Corp. (Palo Alto, CA) was used as calibration standard. The light scattering cell is from VWR

Scientific (Westchester, PA). A He–Ne laser (632.8 nm) is used. Data are taken at 23 °C.

2.4. X-ray Photoelectron Spectrometer (XPS)

The samples prepared for XPS analysis followed the same procedures as for AFM experiments. Before introducing samples into the ultra high vacuum chamber, the samples were further dried in a desiccator for over 24 h. XPS analysis of the surfaces was conducted on a PHI 5500 Spectrometer (Perkin–Elmer) equipped with AugerScan system control (RBD Enterprises), and aluminum $K\alpha$ X-ray radiation source (1486.6 eV) was used. The samples were first placed in a transferring chamber equipped with a Turbo molecular pump. Upon reaching a vacuum of better than $\sim 10^{-7}$ Torr, samples were then transferred to the ultra high vacuum chamber. The pressure in the chamber was below 10^{-8} Torr before the data were taken, and the voltage and current of the anode were 15 kV and 13.5 mA, respectively. Both survey and multiplex spectra were taken from 600 to 0 eV, with a take-off angle of 45°. The pass energies for survey and multiplex scans were 117.40 and 23.50 eV, respectively. The binding energy scale was referenced by setting the C1s peak maximum at 285.0 eV.

2.5. AFM operation

AFM imaging and force measurement were conducted using a Nanoscope IIIa atomic force microscope from Digital Instruments (Santa Barbara, CA) equipped with an E scanner with a maximum scan area of 16 μm^2. The scanner was calibrated following standard procedures provided by Digital Instruments. The fluid cell (Digital Instruments) was washed with deionized water, ethanol, and deionized water before each experiment. Freshly cleaved mica was mounted onto a stainless steel disk using a sticky tab (Latham, NY). After the substrate was brought close to the AFM tip, the freshly prepared EggPC vesicle solution was injected through silicone rubber tubing into the fluid cell, sealed by a silicone rubber O-ring. The EggPC vesicle solution was allowed to incubate on mica at room temperature for 1 h. Excess vesicles were removed by flushing the fluid cell with buffer solution followed by pure water. All images were obtained in pure water because a higher image contrast can be obtained [31]. The microscope was allowed to equilibrate thermally for thirty minutes before imaging. Scanning rate between 1 to 5 Hz and a scanning angle of 0° were used. A setpoint in the range of 0.4–0.6 V was used and free amplitude was adjusted in the range of 0.5–0.8 V. Room temperature was maintained at 22 ± 1 °C. All the images were flattened unless specified.

Images were recorded in contact mode or tapping mode using standard silicon nitride (Si_3N_4) integral tips (NP type), (Digital Instruments) mounted on cantilevers with a manufacturer-specified spring constant of 0.22 N/m, length of 120 μm, width of 15 μm, and a nominal tip radius of curvature between 20 and 40 nm. The radius of the tip 33.20 ± 6.62 nm was calibrated by imaging the TGT01 gratings from Mikromasch Inc. (Portland, OR) [32]. The spring constant of the cantilever was calibrated using the deflection method against a reference cantilever purchased from Park Scientific Instruments Company (Santa Barbara, CA) of known spring constant (0.157 N/m) [33]. The calibrated spring constant 0.17 ± 0.05 N/m was used in all force curves calculations. Force curves were obtained in contact mode only. The total time for a complete cycle was ∼1 s. It is not an easy task to capture force curve directly on the vesicle since the tip radius is comparable to the vesicle radius. Thus, many force curves were obtained on and around the vesicles. However, only the force curve with two jump-in points (i.e., corresponding to the breaking of vesicles) and highest onset point will be accepted for further analysis. As demonstrated in our previous study [28], the force curves with two jump-in points correspond to measurement obtained directly on the vesicle and will represent the interaction between the tip and the vesicles. The force calibration plot is converted to a force versus distance plot by defining the point of zero force and the point of zero separation [34]. Zero force is determined by identifying the region at a large separation, where the deflection is constant. Zero separation is determined from the constant compliance region at high force where deflection is linear with the expansion of the piezoelectric crystal. Only approaching force curves are reported unless otherwise specified.

2.6. Data analysis according to Hertzian model

Our data analysis has been described elsewhere and will only be briefly summarized here [28]. Approaching force distance data was fitted to the Hertzian contact model assuming a spherical shape for the tip [24,27]. The indentation from the difference between the cantilever distance $z - z_0$ and cantilever deflection $d - d_0$ is described in the equation

$$|z - z_0| - (d - d_0) = \delta = A(d - d_0)^{2/3} = 0.825\left[\frac{k^2(R_{\text{tip}} + R_{\text{ves}})(1 - \upsilon_{\text{ves}}^2)^2}{E_{\text{ves}}^2 R_{\text{tip}} R_{\text{ves}}}\right]^{1/3}(d - d_0)^{2/3}, \quad (1)$$

where E_{ves} is the Young's modulus of the vesicle, R_{tip} and R_{ves} are the radius of the tip and vesicle, respectively, υ_{ves} is the Poisson's ratio of the vesicle, and k is the cantilever spring constant. In general, a Poisson's ratio of 0.5 is used for the vesicle to calculate Young's modulus [24,26,35]. The spring constant = 0.17 N/m, and the tip radius = 33 nm are used. The vesicle radius is taken to be equal to $z_0/2$. Experimental data can be fitted to the equation with two fit parameters A and z_0 using SigmaPlot. In general, the fitted z_0 value was found to be consistent with the visually examined contact point. Thus, z_0 in our experiment is determined by the onset point of the repulsive force. E_{ves} is then computed from A (obtained by least square fitting). Only data with indentation (δ) less than 10 nm were used in our calculation to ensure elastic behavior [24]. Bending modulus k_c is

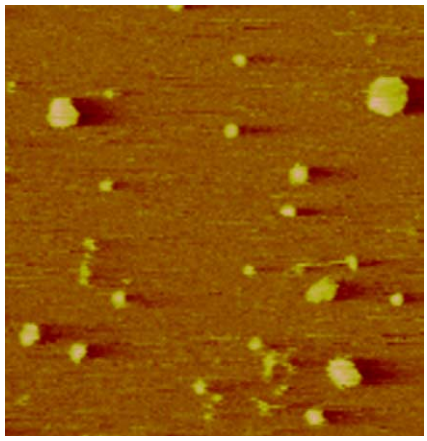

(a)

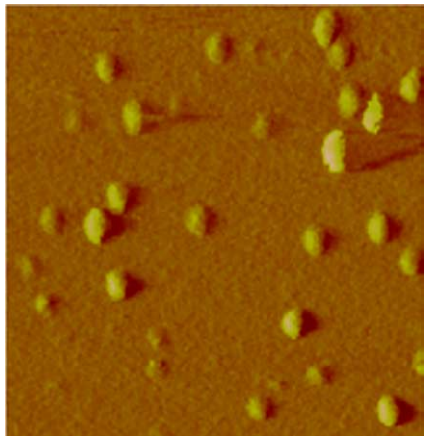

(b)

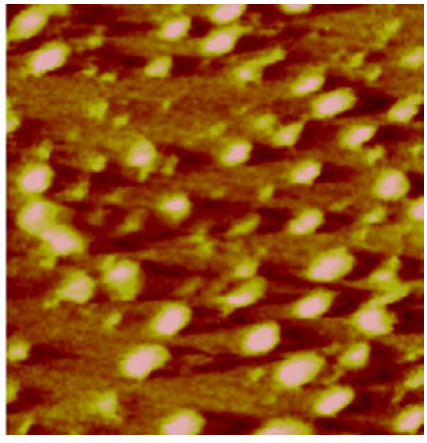

(c)

Fig. 1. AFM amplitude images of liposomes (bright particles) with different molar ratio of cholesterol on mica substrate (dark, flat background) by tapping mode. The vesicle suspension was incubated on mica for 1 h before flushing. The initial EggPC concentration is 0.5 mg/ml. All the images were captured in pure water with images size 0.5 × 0.5 μm, and 20 nm z-scale. The molar ratios of EggPC and cholesterol are: (a) 100:0; (b) 70:30; (c) 50:50.

deduced from Young's modulus based on the equation [36]

$$k_c = \frac{E_{ves} h^3}{12(1-\upsilon_{ves}^2)}, \tag{2}$$

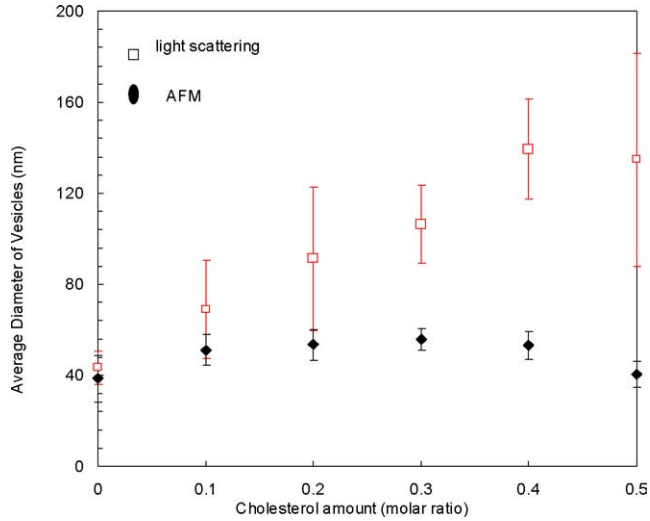

Fig. 2. Liposome size distribution as a function of cholesterol concentration measured in solution by light scattering and on mica substrate by AFM sectional analysis. The error bar from light scattering corresponds to deviation of the vesicle size measured, and the error bar of AFM measurement is the standard deviation of vesicle diameters from a number of vesicles images.

where h is the bilayer thickness. Typically, at least 5 force curves are used to get statistic value of elastic properties.

3. Results and discussion

3.1. Imaging and size determination of liposomes

Tapping mode is known to reduce frictional and adhesive forces that often interfere with imaging of soft samples and therefore is used in this study. Typical amplitude images of the EggPC/cholesterol vesicles with different nominal molar ratio are shown in Fig. 1. It was not possible to make a separate chemical analysis for each individual vesicle adsorbed on mica, so the results are presented in terms of nominal mol% cholesterol. The images resolve individual liposome (spherical particles) on a flat background, which is mica surface.

The average diameters of the particles as measured by AFM images sectional analysis and light scattering were plotted against EggPC/cholesterol nominal molar ratio in Fig. 2. The light scattering shows that the sizes of the liposomes increased with the incorporation of cholesterol, as is consistent with the literature [12,14]. While, a relatively constant size around 40–60 nm was observed by AFM sectional analysis regardless of different EggPC/cholesterol ratios. The diameter of the particles was measured based on tapping mode image sectional analysis. Tip convolution effect on vesicle size by tapping mode is not significant as compared to contact mode as reported [28]. Possible explanations for the apparent inconsistently values are postulated as follows. For light scattering, the technique gives the average bulk values of the size distributions in solu-

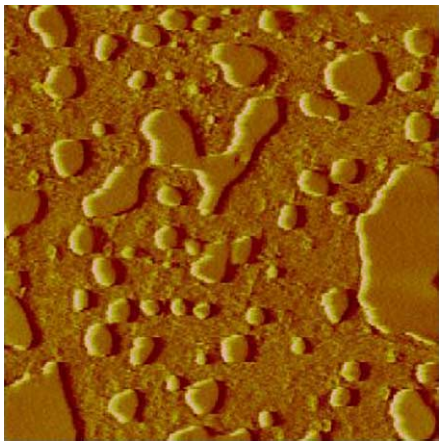

Fig. 3. AFM amplitude images of liposomes and bilayer patches on mica substrate by tapping mode. The nominal molar ratio of EggPC and cholesterol is 90:10. The bilayer patches are formed from the rupture of big size vesicles upon adsorption. The image size is 1×1 μm, and 20 nm z-scale.

tion. Some extra large vesicles in the solution will affect the size distribution dramatically; on the other hand, AFM measured the adsorbed vesicles on mica surface. It is unlikely that every vesicle–surface interaction results in adhesion upon adsorption [31]. Large vesicles may rupture upon adsorption, and are more easily disrupted during AFM scanning [29]. Fig. 3 shows the bilayer and vesicles coexistent for EggPC/cholesterol (nominal 10% cholesterol molar ratio) system observed by AFM imaging. The bilayer probably formed after the big vesicles ruptured upon adsorption. The majority bilayer sizes in Fig. 3 are in the range of 120–180 nm which corresponded to the rupture of vesicles with 60–90 nm diameter. The biggest bilayer in the image was probably due to the fusion, then rupture of very big vesicles. On the other hand, small vesicles have shown to be stable upon adsorption [29]. Therefore, it is possible that only liposomes below certain critical sizes that are stable upon adsorption on mica can be observed by AFM on mica. In this case, the apparent critical size of modified liposomes is in the range of 40–60 nm. Another possibility is that, before we image the vesicles, we use pure water to drive away drifting vesicles (which are not adsorbed on the substrate; sometimes drifting vesicles can stack on top of the adsorbed vesicles), or some bigger vesicles (which are not very stable on the substrate).

Light scattering and AFM imaging can provide sizes and size distributions of free vesicles in solution and supported vesicles on substrate, respectively. Both techniques clearly reveal the difference of cholesterol-modified vesicles under these conditions. The critical question is to determine whether these adsorbed vesicles exhibit different micro-mechanical properties. Thus, our next step is to conduct force measurements on individual adsorbed vesicles prepared from different nominal cholesterol ratios, because cholesterol is known to alter the mechanical properties of liposomes.

3.2. Elastic properties analysis

The force curves between an AFM tip and an adsorbed vesicle are obtained in contact mode. In our experiments, we found that the retracting force curve is quite complicated because it involves the resealing of portions of the bilayer and the adhesion force between the tip and the vesicles upon retraction. On the other hand, the approaching force curve provides a wealth of stepwise micromechanical deformation events on the liposomes. Thus, only the approaching force curves are shown here. Fig. 4a shows a typical deflection versus z position plot on a vesicle containing cholesterol (EggPC 80:cholesterol 20). Fig. 4b is a force versus distance curve based on the data from Fig. 4a by defining the zero force and zero separation point. This force curve shares many similarities with those obtained on pure EggPC vesicles [28].

Figs. 4a and 4b can be divided into four regions as labeled. In region I, the non-contact region, the tip is far away from vesicle and the force between the tip and the vesicle is zero. Region II illustrates the elastic deformation of the vesicle under tip compression and therefore can be used to calculate the Young's modulus. Region III corresponds to further tip compression after the tip penetrates the vesicle's top bilayer. Region IV reflects the cantilever deflection when it is in contact with the hard mica substrate after penetrating through the vesicle's bottom bilayer. Theoretically, the slope of region IV in Fig. 4a should be 1.0 because the deflection of the cantilever is identical to the z direction movement of sample on hard surface [21]. Based on the fitted data, a slope of 0.9967 ± 0.0036 was obtained. The two jump-in points during the rise of the steric repulsion correspond to the tip penetrating the upper (which vesicle bilayer is in direct contact with the tip) and lower portion (which vesicle bilayer is resting on mica) of each vesicle, respectively [28]. A recent study suggested AFM tip is covered by a lipid bilayer that may affect the interpretation of various tip-vesicle interaction phenomena observed. However, in our system, there is one main difference in the force curve obtained on bilayer compared with the force curve reported by Richter and Brisson [37]. Our data showed the onset of repulsive regime on EggPC bilayer occurs at a separation of (6.58 ± 0.37 nm) [28], while, a separation of $\sim$9 nm was reported in their study. Thus, our data support that there is no lipid bilayer adsorbed on tip. To further support our conclusion that no bilayer was adsorbed on the tip, the following force curve measurements on mica were conducted. The first measurement was with a clear tip in pure water, while the other measurement was with a tip that has been in the vesicle solution environment for an hour. We found essentially no difference in the force curves obtained suggesting no lipid bilayer was adsorbed on the tip under our experiment conditions.

The slope of a force curve describes the elastic properties of a sample in a qualitative way [21,24]. The slope values of the first repulsive region II and second repulsive region III

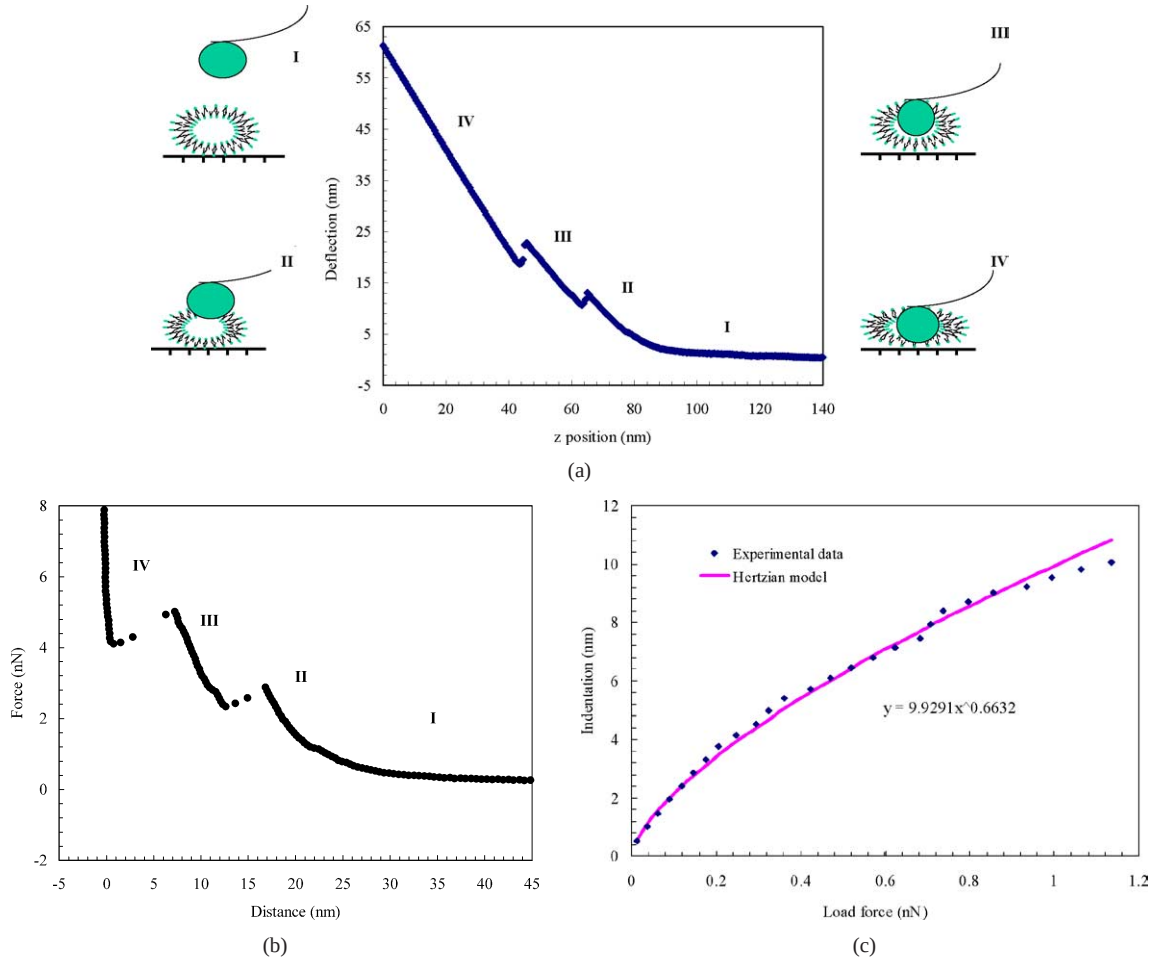

Fig. 4. (a) Deflection versus z position approaching curve. The point of zero force is defined while the point of zero separation is not defined as described previously. The force curve is obtained on the EggPC/cholesterol liposome with molar ratio 80:20. x-axis represents z position (z scan size) and y is cantilever deflection. There are four regions. Region I is non-contact. Regions II–IV illustrate different on-contact stages of tip and sample interaction. Region II illustrates the elastic deformation of the vesicle under tip compression. Region III corresponds to further tip compression after the tip penetrating the top bilayer. Region IV shows the tip is on the top of mica substrate, a steep slope 0.9946 indicates mica is an infinitely hard surface without deformation; (b) A typical force curve on an EggPC/cholesterol liposome based on the data from (a) by defining the zero force and zero separation point; (c) Force curve data fit with Hertzian model for region II in (a). The squares are experimental data. Experimental data can be described by power equation $\delta = 9.9291F^{0.6632}$. The solid line is the Hertzian model $\delta = AF^{2/3}$ with $A = 9.9291$. It shows there is a good agreement between the experimental findings and the Hertzian model.

Table 1
Slope of the repulsive forces on the liposomes

Sample (EggPC:chol molar ratio)	100:0	85:15	80:20	70:30	50:50
Slope of 1st repulsive force (N/m)	0.04 ± 0.02	0.18 ± 0.07	0.24 ± 0.07	0.20 ± 0.09	0.15 ± 0.04
Slope of 2nd repulsive force (N/m)	0.19 ± 0.08	1.27 ± 0.63	0.49 ± 0.22	0.53 ± 0.23	1.34 ± 0.38

before and after the first breakthrough point for different molar ratio EggPC/cholesterol systems are listed separately in Table 1. The values lay in the range of 0.15 to 0.24 and 0.49 to 1.34 N/m for the EggPC/cholesterol vesicles. By comparison, the slope values for the pure EggPC vesicles of the two repulsive force regimes are 0.04 ± 0.02 and 0.19 ± 0.08 N/m, respectively, significantly lower than those containing cholesterol. By fitting our experimental data (region II and region III) to Hertzian model $\delta = AF^b$ (where F is loading force) we obtained exponent b of 0.6632 (region II) and 0.9227 (region III), respectively. The poor fit on the high loading force (region III) ($b = 0.9227$) suggested that the Hertzian model severely fails in region III. The exponent $b = 0.6632$ which is close to the $2/3$ in region II is remarkable. Although Hertzian model describes the contact between two solid bodies on the basis of continuum elasticity theory without adhesion force [27], the good fit in region II suggests that Hertzian model may also be applicable to describe the elastic deformation between the tip and the vesicle within the limit of small indentation. Region II (Figs. 4a and 4b)

Table 2
Comparison of Young's modulus E and bending modulus (k_c) of liposome with different cholesterol and lipid ratio

Sample	Pure EggPC	85:15	80:20	70:30	50:50
$E \times 10^6$ Pa	1.97 ± 0.75	12.07 ± 1.53	10.77 ± 0.64	10.4 ± 4.06	13.0 ± 2.97
$k_c \times 10^{19}$ (J)	0.27 ± 0.10	1.68 ± 0.21	1.49 ± 0.09	1.44 ± 0.56	1.81 ± 0.41

illustrates the elastic deformation of the vesicle under tip compression, thus, all subsequent calculations for determining the micromechanical properties of the vesicle surfaces employed the data in region II based on Hertzian model.

Fig. 4c is the indentation versus load force based on the data from Fig. 4a region II. It shows there is a good agreement between the experiment findings and the Hertzian model.

The Young's modulus and bending modulus k_c of the tested liposomes were calculated using Eqs. (1) and (2) with bilayer thickness $h = 5 \times 10^{-9}$ m. It should be noted that the value of Young's modulus is slightly affected by the value of Poisson's ratio (e.g., a 10% deviation of Poisson's ratio from 0.5 to 0.45 causes a 6% increase of Young's modulus). On the other hand, the bending modulus would not be affected by Poisson's ratio variation. The values are reported in Table 2. It is clear that the bending modulus of liposome increased with cholesterol incorporation.

3.3. Cholesterol effect on mechanical properties of liposomes

Table 2 lists the Young's modulus and bending modulus of EggPC/cholesterol systems with different molar ratio calculated based on AFM approaching force curves. Compared with pure EggPC, the Young's modulus and bending modulus of the modified liposome were found to increase significantly. It is plausible that the significant elastic properties change is due to cholesterol. It has been reported that the phospholipid bilayer packing geometrical structures have been changed after cholesterol incorporation [12] and thus can enhance fluidity and intravesicle interaction. After the cholesterol is incorporated into phospholipid bilayers, the small hydrophilic 3β-hydroxyl head group of cholesterol is located in the vicinity of the lipid ester carbonyl groups, and the hydrophobic steroid ring orients itself parallel to the acyl chains of the lipid [38]. Thus, the movement of the acyl chains of the phospholipid bilayer has been restricted. Below the gel phase transition temperature (T_m) of lipids, cholesterol addition increases the fluidity of lipids, while above T_m the mobility and fluidity of the lipid chains are restricted (T_m of EggPC is $-15\,^\circ$C) [1]. Moreover, hydrogen bonding between cholesterol's β-OH and the carbonyl groups of the lipid enhances the stability of the bilayer [10]. The interaction between the cholesterol and phospholipid bilayer results in an increase in membrane cohesion, as shown by increases in the mechanical stiffness of the membranes. Thus, the vesicle rigidity is determined by the cholesterol content (See Table 3). Table 3 listed bending modulus comparison of PC/cholesterol systems studied by different groups and methods.

An increase of bending modulus (k_c) is expected as nominal cholesterol fraction increases, and a clear trend was observed for DMPC/chol system [18,19] in solution. Evans et al. [20] compared stearoyloleoylphosphatidylcholine (SOPC) and SOPC:chol (1:1 mixture of SOPC and cholesterol) and found that the bending modulus is $(0.9 \pm 0.06) \times 10^{-19}$ and $(2.46 \pm 0.39) \times 10^{-19}$ J, respectively. The bending modulus of liposomes was increased up to 3 times by cholesterol incorporation (Table 3). In addition to bending modulus, a nonlinear increase in elastic area compressibility expansion modulus (k_a) (which is proportional to the bending modulus) with increasing amounts of cholesterol up to a constant plateau (a cholesterol concentration above 50%) was observed for a series of SOPC/chol systems [15]. It is obvious that the elastic properties of lipid/cholesterol systems increased with cholesterol amount increased in bulk solution.

EggPC used in this study is a phospholipid extracted from egg yolk. Its hydrocarbon chains have different lengths and different degrees of unsaturation. EggPC consists of fatty acid with different chain lengths. Fatty acid chain length is also the important factor that determines the stability of vesicles. EggPC at room temperature is liquid crystalline because its T_m is $-15\,^\circ$C [1]. Since EggPC has, on the average, a similar hydrocarbon chain composition to SOPC, we assume that the energy of adhesion is similar for EggPC/chol and SOPC/chol bilayers. The bending rigidity should scale as the area compressibility modulus times the membrane thickness squared ($k_c \sim k_a h^2$) [20]. It has been shown that cholesterol substantially increases the area compressibility and the derived bending modulus of bilayers. Using the estimated hydrocarbon thickness for pure EggPC and published values of the compressibility moduli for SOPC/chol bilayers, we can estimate that the incorporation of cholesterol increases k_c by a factor of 1.54, 1.97, 2.59, and 6.15 for 15, 30, 40, and 50% of cholesterol, respectively. Note that this calculation is based on vesicles in bulk solution.

Our data did not show similar increases in the bending modulus as a function of nominal cholesterol amount (Table 2). The bending modulus of EggPC/chol system increased by 5–6 times compared with pure EggPC regardless of the nominal cholesterol amount. Table 2 shows that the significant increment occurred while reaching a plateau. The change of elastic properties was consistent with the slope of the force curve (Table 1) with a plateau (Slope of 1st repulsive force).

Table 3
Bending modulus comparison of phosphatidylcholine (pc) containing cholesterol

Composition (PC/chol)	Bending modulus $k_c \times 10^{19}$ (J)	Method	Vesicle size	Temperature (°C)	Ref.
DMPC/chol		Phase contrast microscopy	Giant quasispherical vesicles	30	[18]
100/0	1.30 ± 0.08				
90/10	2.00 ± 0.1				
70/30	4.1 ± 0.25				
50/50	6.1 ± 0.3				
DMPC/chol		Phase contrast microscopy	Giant quasispherical vesicles	40	[18]
100/0	1.27 ± 0.09				
90/10	1.84 ± 0.09				
70/30	3.07 ± 0.13				
50/50	3.7 ± 0.3				
DMPC/chol		Phase contrast microscopy	Giant vesicles (∼10 μm)	30	[19]
100/0	1.15 ± 0.15				
80/20	2.1 ± 0.25				
70/30	4.0 ± 0.8				
SOPC/chol		Micropipette method	∼20 μm		
100/0	0.90 ± 0.06			18	[20]
50/50	2.46 ± 0.39			15	
EggPC/chol		AFM force curve method	<60 nm	22 ± 1	This work
100/0	0.27 ± 0.10				
85/15	1.68 ± 0.21				
80/20	1.49 ± 0.09				
70/30	1.44 ± 0.56				
50/50	1.81 ± 0.41				

* DMPC: dimyristoylphosphatidylcholine; SOPC: stearoyloleoylphosphatidylcholine.

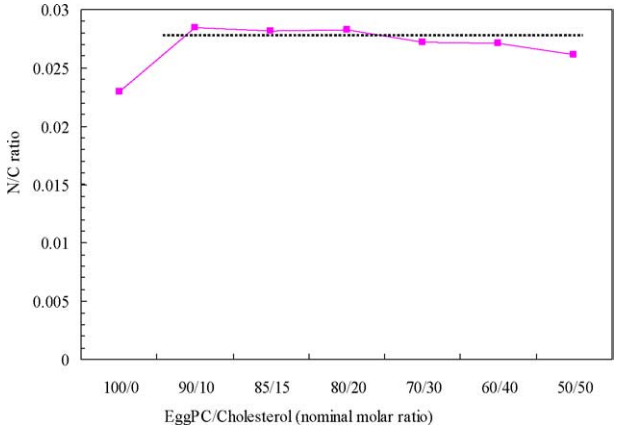

Fig. 5. The atomic concentration ratio of nitrogen with respect to total carbon (N/C) as a function of the cholesterol amount by XPS. The N/C atomic concentration ratio reached a plateau.

Possible reasons for this are postulated as following. As discussed earlier, vesicle size fell into the 40–60 nm range despite the presence cholesterol on the substrate, as indicated by AFM imaging. Thus only vesicles in a certain critical size range remained adsorbed on mica surface, and vesicles of a certain size are expected to contain a certain amount of cholesterol, and thus to have similar elastic properties. To further investigate the composition of adsorbed vesicles, the surface chemical composition of EggPC/chol was analyzed by X-ray photoelectron spectrometry (XPS). The nitrogen atomic concentration ratio with respect to total carbon as a function of nominal cholesterol amount is shown in Fig. 5. Theoretically, the N/C atomic concentration ratio increases with the amount of EggPC. However, the experimental data showed that the N/C ratio reached a plateau after cholesterol incorporation, independent of the nominal cholesterol amount. Thus, it agrees with our explanation for the relatively constant elastic properties of EggPC/chol systems. From Fig. 2, a plateau of supported EggPC/cholesterol vesicle size was also observed after cholesterol incorporation by AFM. Thus, it is acceptable to assume that vesicles above 100 nm in diameter tend to be unstable and to form bilayers (Fig. 3) upon adsorption. Furthermore, it was reported that the bending modulus is proportional to vesicle size [39–41]. In this study, the bending modulus measured by AFM force curve also shows the same trend. Fig. 6 showed the relationship between bending modulus and vesicle size for both pure and cholesterol-modified EggPC. In AFM experiment, the ability to image and then determine micro-mechanical properties in exactly the same location is extremely difficult. In order to provide a direct correlation of vesicle size and bending modulus, the vesicle size for Fig. 6 is determined by using the onset point of first repulsive regime [24,28]. Onset point of repulsive force is proportional to vesicle size and it is usually smaller than vesicles size measured by lateral dimension because of flattening of vesicles upon adsorption [24,28]. The term “nominal vesicle size” (onset point of repulsive force) was used to in Fig. 6 to distinguish from

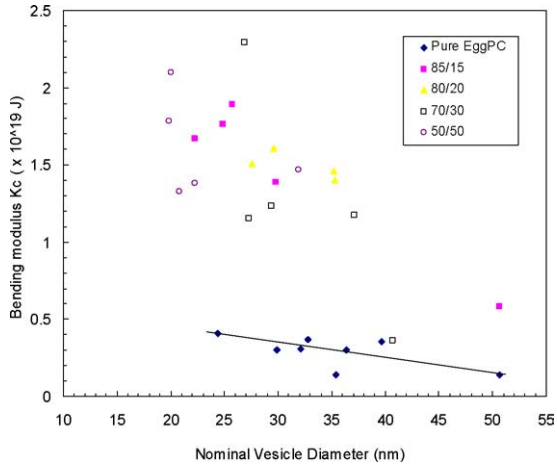

Fig. 6. The relationship between bending modulus and nominal vesicle size. The vesicle size was determined by onset point of first repulsive force, and nominal vesicle size was used to distinguish from vesicle size measured based on lateral dimension. The straight line was used to guide eye. Two trends were observed. One is the bending modulus decreased with vesicle size increase. The other one is the bending modulus of vesicles containing cholesterol was higher than that of pure EggPC when the vesicle size is the same.

vesicle size measured based on lateral dimension (Fig. 2). Clearly, the bending modulus measured decreased with vesicle size increase. The results also suggested that rupture of vesicles containing high molar ratio (with larger vesicle size from light scattering) happens upon adsorption, only vesicle below certain critical size is stable. On the other hand, it was obvious that the bending modulus of vesicle containing cholesterol is significantly higher than that of pure EggPC for the same vesicle size.

As discussed above, the bending modulus of EggPC/cholesterol is estimated to increase k_c by a factor of 1.54, 1.97, 2.59, and 6.15 for 15, 30, 40, and 50% of cholesterol, respectively, in bulk solution. While, our data shows an approximately 5–6 factor increase for supported EggPC/cholesterol. The reason for the inconsistency is probably due to the fact that our data were obtained on the adsorbed vesicles.

4. Summary

In this study, the Young's modulus (E) and the bending modulus (k_c) for small unilamellar vesicles on substrate are quantified by analyzing AFM approach force curves based on Hertzian model. It was found that the Young's modulus and bending modulus increased by several times after the cholesterol incorporation into pure EggPC. The significant difference is attributed to the enhanced rigidity of the EggPC vesicles as a result of the incorporation of cholesterol molecules. There is a critical size for vesicles adsorbed on mica substrate; thus, no similar trend of elastic properties is observed as a function of nominal cholesterol fraction as that in solution. The results indicate that the AFM can provide a direct method to measure the mechanical properties of immobilized small liposomes and to detect the stability change of liposomes. The result also showed that the stability of liposomes on substrate is significantly different from that in solution. These results are important since the adhesion of vesicles represents an essential step for mass transfer through large membrane.

Acknowledgments

We wish to thank the donors of the Petroleum Research Fund 36149-ACS and 33036-ACS administered by the American Chemical Society, Michigan Life Science Corridor, and the Institute for Manufacture Research in Wayne State University for the financial support. We also thank Jerome S. Jourdan at BASF Wyandotte, Michigan for help with the light scattering measurement. Lastly, our thanks to Professor Sandro R.P. da Rocha for his constructive comments on the manuscript.

References

[1] R.R.C. New, in: R.R.C. New (Ed.), Liposomes: A Practical Approach, Oxford Univ. Press, New York, 1990.
[2] Y. Barenholz, Curr. Opin. Colloid Interface Sci. 6 (2001) 66.
[3] D.D. Lasic, Tibtech 16 (1998) 307.
[4] D.D. Lasic, D. Papahadjopoulos, Science 217 (1995) 1245.
[5] K. Sou, T. Eudo, S. Takeoka, E. Tsuchida, Bioconjugate Chem. 11 (2000) 372.
[6] K. Kono, A. Henmi, H. Yamashita, H. Hayashi, T. Takagishi, J. Controll. Release 59 (1999) 63.
[7] M. Johnsson, N. Bergstrand, K. Edwards, J.J.R. Stålgren, Langmuir 17 (2001) 3902.
[8] K. Kostarelos, M. Kipps, Th.F. Tadros, P.F. Luckham, Colloids Surf. A 136 (1998) 1.
[9] K. Kostarelos, Th.F. Tadros, P.F. Luckham, Langmuir 15 (1999) 369.
[10] F.T. Presti, R.J. Pace, S.I. Chen, Biochemistry 21 (1982) 3831.
[11] M.G. Virden, J.C. Berg, Langmuir 8 (1992) 1532.
[12] D. Liu, W. Chen, L. Tsai, S. Yang, J. Chin. Inst. Chem. Engrs. 31 (2000) 269.
[13] R.P. Rand, V.A. Parsegian, J.A.C. Henry, L.J. Lis, M. Mcalister, Can. J. Biochem. 58 (1980) 959.
[14] D. Liu, W. Chen, L. Tsai, S. Yang, Colloids Surf. A 172 (2000) 57.
[15] D. Needham, R.S. Nunn, Biophys. J. 58 (1990) 997.
[16] S. Svetina, B. Zeks, in: D.D. Lasic, Y. Barenholz (Eds.), Handbook of Nonmedical Applications of Liposomes, CRC Press, Boca Raton, FL, 1996, chap. 1.
[17] R.M. Servus, W. Harbich, W. Helfrich, Biochim. Biophys. Acta 436 (1976) 900.
[18] P. Meleard, C. Gerbeaud, T. Pott, L. Fernandez-Puente, I. Bivas, M.D. Mitov, J. Dufourcq, Biophys. J. 72 (1997) 2616.
[19] H.P. Duwe, E. Sackman, Physica A 63 (1990) 410.
[20] E. Evans, W. Rawicz, Phys. Rev. Lett. 64 (1990) 2094.
[21] A.L. Weisenhorn, M. Khorsandi, S. Kasas, V. Gotzos, H.-J. Butt, Nanotechnology 4 (1993) 106.
[22] H.-J. Butt, M. Jaschke, W. Ducker, Bioelectrochem. Bioenerg. 38 (1995) 191.
[23] A. Ikai, K. Mitsui, H. Tokuoka, X. Xu, Materials Sci. Eng. C 4 (1997) 233.

[24] D.E. Laney, R.A. Garcia, S.M. Parsons, H.G. Hansma, Biophys. J. 72 (1997) 806.
[25] I. Lee, R.E. Marchant, Colloids Surf. B 19 (2000) 357.
[26] M. Radmacher, M. Fritz, C.M. Kacher, J.P. Cleveland, P.K. Hansma, Biophys. J. 70 (1996) 556.
[27] M. Radmacher, M. Fritz, C.M. Kacher, D.A. Walters, P.K. Hansma, Langmuir 10 (1994) 3809.
[28] X. Liang, G. Mao, K.Y.S. Ng, Colloids Surf. B 34 (2004) 41.
[29] I. Reviakine, A. Brisson, Langmuir 16 (2000) 1608.
[30] C.-H. Huang, Biochemistry 8 (1969) 344.
[31] Z.K. Leonenke, A. Carnini, D.T. Cramb, Biochim. Biophys. Acta 1509 (2000) 131.
[32] J.S. Villarrubia, J. Res. Natl. Inst. Stand. Technol. 102 (1997) 425.
[33] M. Tortonese, M. Kirk, SPIE 3009 (1997) 53.
[34] C.B.Prater, P.G. Maivald, K.J. Kjoller, M.G. Heaton, Probing Nanoscale Forces with Atomic Force Microscope, vol. 8, Digital Instruments, 1995, and references therein.
[35] M. Heuberger, G. Dietler, L. Schlapbach, Nanotechnology 5 (1995) 12.
[36] E.A. Evans, Biophys. J. 14 (1974) 923.
[37] R.P. Richter, A. Brisson, Langmuir 19 (2003) 1632.
[38] B.D. Ladbrooke, R.M. Williams, D. Chapan, Biochim. Biophys. Acta 150 (1968) 333.
[39] G. Niggemann, M. Kummrow, W. Helfrich, J. Phys. France 5 (1995) 413.
[40] I. Bivas, P. Hanusse, P. Bothorel, J. Lalanne, O. Aguerre-Chariol, J. Phys. France 48 (1987) 855.
[41] M.B. Schneider, J.T. Jenkins, W.W. Webb, J. Phys. France 45 (1984) 145.